

Backscattering of circularly polarized pulses

Arnold D. Kim

Department of Mathematics, Stanford University, Stanford, California 94305-2125

Miguel Moscoso

Departamento de Matemáticas, Escuela Politécnica Superior, Universidad Carlos III de Madrid, Avenida de la Universidad 30, 28911 Leganés, Spain

Received April 30, 2002

Using numerical simulations of vector radiative transport, we examine time-resolved backscattering of circularly polarized plane waves normally incident upon a slab containing a random distribution of latex spheres in water. For large spheres the effect of polarization memory occurs a short time after first-order scattering and before depolarization. It is the result of successive near-forward-scattering events that maintain the incident wave's helicity. For moderately large scatterers it exhibits a simple dependence on the anisotropy factor. For larger spheres or those with higher refractive indices, it also depends on complicated angular and polarization characteristics of backscattering given by Mie theory. © 2002 Optical Society of America

OCIS codes: 260.5430, 290.4210, 030.5620, 290.1350.

Among the several studies of the propagation of polarized light in multiply scattering media,¹⁻⁴ it has been demonstrated that backscattered circularly polarized light exhibits a peculiar behavior. More specifically, let us consider a medium containing a random distribution of dielectric spheres bounded by two parallel planes. A circularly polarized wave impinges upon one of the boundaries normal to the boundary plane. If backscattered light is not depolarized, one anticipates that it will consist mainly of the circular polarization state corresponding to that which would result from specular reflection by a perfectly conducting plate. However, this intuition is correct only for spheres whose radii are smaller than the wavelength. For larger spheres the opposite situation obtains. This unexpected memory of the incident circular polarization is called polarization memory.¹ Here we examine polarization memory by studying the temporal behavior of backscattered circularly polarized light.

To model propagation of polarized light in a multiply scattering medium we use the theory of radiative transport. This theory assumes that scattered fields from different scatterers are uncorrelated, so coherent backscattering effects are not modeled. We compute solutions of the time-dependent vector radiative transport equation, using the Chebyshev spectral method.⁵ We consider a left-handed circularly polarized plane-wave pulse normally incident upon an index-matched, plane-parallel medium containing a random distribution of dielectric spheres, each with radius a and relative refractive index m . Ishimaru *et al.*⁶ provide a complete formulation of this problem.

We consider latex spheres in water such that the relative refractive index of the spheres is $m = 1.19$. The wavelength is $\lambda = 633$ nm, so the wave number in water is $k = 13.21 \mu\text{m}^{-1}$. The incident pulse is Gaussian, with unit height and width $T = 0.01L/c$, where L is the thickness of the slab and c is the constant wave speed in the medium. We fix the optical thickness of the slab at $\tau_0 = 10$. We have observed results similar to those presented here for different optical thick-

nesses, provided that sufficient multiple scattering was allowed for.

In Fig. 1 we plot the time-resolved backscattered fluxes on a time scale normalized by $t_0 = L/c$ for spheres with size parameters $ka = 1.0, 2.5, 4.0$. These fluxes were computed for a full field of view. Time is calibrated such that $t = 0$ corresponds to the time at which the peak of the incident pulse enters the medium. The left-handed and right-handed circularly polarized components are plotted as solid and dashed curves, respectively. We define the helicity of polarization with respect to the direction of propagation. Then, according to this definition, a left-handed circularly polarized wave is specularly reflected as a right-handed circularly polarized wave by a perfectly conducting plate.

Except for the smallest spheres shown in Fig. 1(a), the left-handed circularly polarized component becomes larger than the right-handed component after a short time; this phenomenon is polarization memory. Details of this development appear in the insets of Figs. 1(b) and 1(c). The left-handed circularly polarized component eventually reaches a maximum, after which it decreases until the difference between the two circularly polarized components becomes negligible. Circular depolarization occurs after a sufficiently large number of scattering events has occurred⁴ and can be seen in the tails of all the backscattered fluxes in Fig. 1.

Inasmuch as the medium is optically thick, a fraction of backscattered flux is made up of waves that have been redirected as backscattering after successive scattering events at near-forward angles. For larger spheres the anisotropy factor g is nearly 1, which means that, after one scattering event, most of the light is scattered in a small area in the forward direction. This scattered light also largely maintains the same circular polarization as that of the incident wave. Hence, for $g \sim 1$, these near-forward-scattered waves make up a significant portion of the backscattered flux and appear as polarization memory. By causality, these waves travel over a finite distance

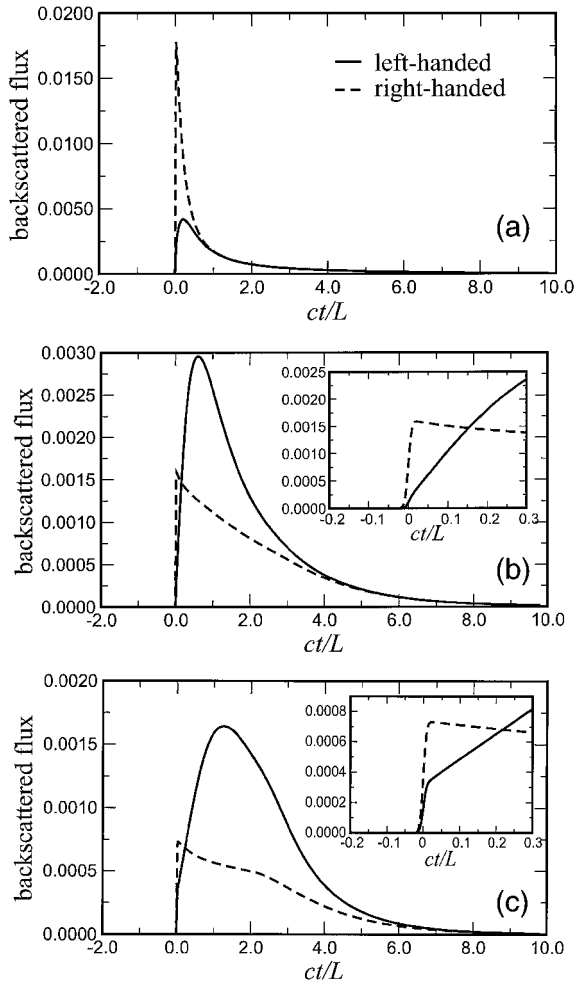


Fig. 1. Backscattered flux as a function of time for spheres with $ka =$ (a) 1.0, (b) 2.5, (c) 4.0. Time is normalized by c/L , where c is the constant wave speed and L is the length of the slab. The incident wave is a left-handed circularly polarized pulse of width $0.01L/c$. The insets in (b) and (c) show details on a shorter time scale near $t = 0$.

before emerging from the medium as backscatter light. Therefore a finite time elapses before polarization memory appears.

Our numerical data support this interpretation. In Fig. 1(a) polarization memory is not seen because the anisotropy factor ($g = 0.41$) is too small to support this effect. The larger spheres shown in Figs. 1(b) and 1(c) have $g = 0.74$ and $g = 0.86$, respectively. For these spheres the right-handed circularly polarized component is larger than the left-handed component for a short time after $t = 0$. These early responses arise from first-order backscattering in which the spheres act as a perfectly conducting plate, reversing the helicity of the waves. As time elapses, those near-forward-scattered waves that have been redirected as backscattering appear. They dominate the backscattered response because they carry a relatively large fraction of power. The smaller the neighborhood of forward scattering, the larger the number of scattering events that are needed for light to be redirected as backscattering. Hence, more time elapses before this effect occurs. For example, the $ka = 4.0$ case shows

a longer delay of the left-handed circularly polarized component's peak than for $ka = 2.5$. We examined the peak time t_{peak} of the left-handed circularly polarized component as a function of g for sphere sizes in the range $2.0 \leq ka \leq 6.0$. From these data we computed the least-squares fit to a quadratic in g . A plot of these results appears in Fig. 2 and shows excellent agreement between the data and the fitted curve.

This quadratic dependence of t_{peak} on g is not universally true, however. For example, computing t_{peak} for $ka > 6.0$ or, instead, the same-sized spheres with $m = 1.40$ (neither case is shown here) produces qualitatively different results with no clear dependence on g . To understand why this is so, we examined scattering by a single sphere, using Mie theory. When $m = 1.40$, for example, g does not grow monotonically for $2.0 \leq ka \leq 6.0$; it fluctuates for $ka > 3.0$. Apart from the large component of near-forward angles characterized by g , the angular distribution and circular polarization characteristics of scattering for these spheres are more complicated. In Fig. 3 we plot Stokes parameter V computed by Mie theory as a function of the cosine of the scattering angles Θ that correspond to backscattering for $m = 1.19$ and $m = 1.40$ for spheres with $ka = 3.0$ (dotted curves), $ka = 4.0$ (solid curves), and $ka = 5.0$ (dashed curves). The incident plane wave that we used to compute this quantity is left-handed circularly polarized with unit power. A positive value of V corresponds to left-handed circularly polarized light. It is this significant portion of helicity-preserving ($V > 0$) backscattered light in these plots for $m = 1.40$ that complicates the relationship between t_{peak} and g . Similar results occur for $m = 1.19$ and $ka > 6.0$. For example, radiative transport with $m = 1.19$ and $ka = 9.24$ [Fig. 4(a)] and $m = 1.40$ and $ka = 5.28$ [Fig. 4(b)] produces a left-handed circularly polarized component that is larger than the right-handed component in the backscattered flux for all times until depolarization. These helicity-preserving, first-order backscattered waves given by Mie theory are the reason for this phenomenon.

By examining time-resolved backscattering of circularly polarized pulses we explain polarization memory: It is the result of successive near-forward scatterings enhanced by a large anisotropy factor. It occurs during the transition between first-order scattering and diffusion. Because a directional description is

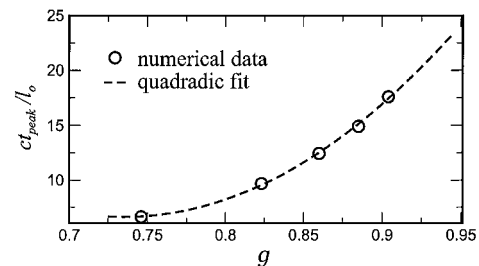


Fig. 2. Peak time t_{peak} of the left-handed circularly polarized component as a function of anisotropy factor g and its least-squares fit to a quadratic in g ($ct_{\text{peak}}/l_0 \approx 380.23g^2 - 559.23g + 212.23$). These times are normalized by l_0/c , where l_0 is the scattering mean free path.

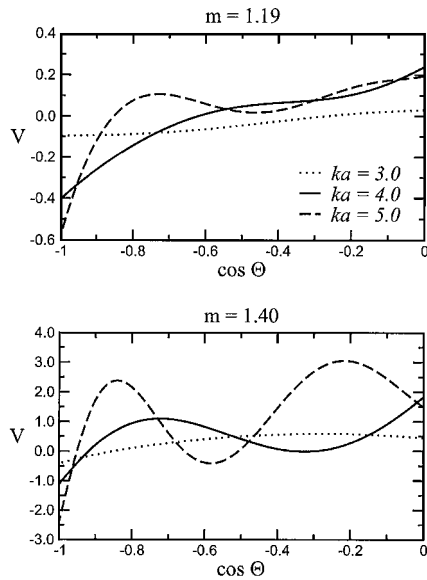


Fig. 3. Stokes parameter V computed by Mie theory for $m = 1.19$ and $m = 1.40$ plotted as a function of the cosine of scattering angle Θ for backscattering. Three sphere sizes are plotted: $ka = 3.0, 4.0, 5.0$.

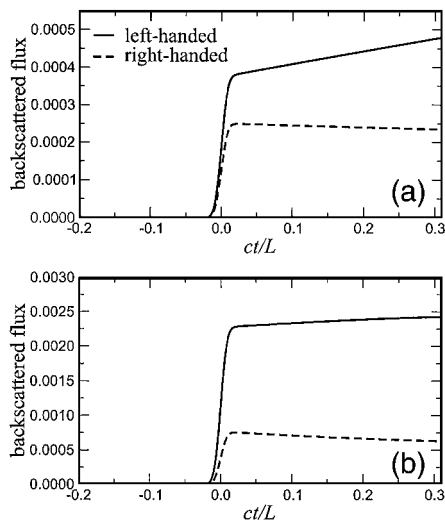


Fig. 4. Same as Fig. 1 for (a) $m = 1.19$ and $ka = 9.24$ and (b) $m = 1.40$ and $ka = 5.28$.

needed to explain it, polarization memory cannot be adequately explained by the diffusion approximation. Hence, polarization memory alone does not indicate

disparate diffusion and depolarization length scales because it takes place, spatially and temporally, before both of these phenomena. Because our computations are made on the basis of radiative transfer, the phenomenon that we observe is not the result of any coherent backscattering effects. For very large-sized or high-contrast spheres, the extent to which polarization memory occurs (i.e., the peak time) cannot be explained through the value of the anisotropy factor alone and requires closer examination of the underlying Mie theory. Regardless, polarization memory strongly depends on g . We observe polarization memory in our computations for relatively small scatterers ($ka \geq 2.5$), indicating that the amount of anisotropy needed is not large ($g \geq 0.7$). We anticipate that this explanation for polarization memory will hold for other multiply scattering media with forward peaked scattering. A careful analysis of the polarization characteristics in anisotropic scattering media^{7,8} by use of the Fokker-Planck approximation should reveal the balance among multiple scattering, anisotropy, and polarization and is a subject of our projected future research.

A. D. Kim acknowledges support from National Science Foundation mathematical sciences postdoctoral fellowship DMS-0071578. M. Moscoso acknowledges support from Dirección General de Enseñanza Superior grant PB98-0142-C04-01 from the Autonomous Region of Madrid (Strategic Groups Action) and from grant RTN2-2001-00349 from the European Union. A. D. Kim's e-mail address is adkim@math.stanford.edu.

References

1. F. C. MacKintosh, J. X. Zhu, D. J. Pine, and D. A. Weitz, *Phys. Rev. B* **40**, 9342 (1989).
2. D. Bicut, C. Brosseau, A. S. Martinez, and J. M. Schmitt, *Phys. Rev. B* **49**, 1767 (1994).
3. E. E. Gorodnichev, A. I. Kuzovlev, and D. B. Rogozkin, *JETP Lett.* **68**, 22 (1998).
4. A. D. Kim and M. Moscoso, *Phys. Rev. E* **64**, 026612 (2001).
5. A. D. Kim and M. Moscoso, *SIAM J. Comput. Sci.* **23**, 2075 (2002).
6. A. Ishimaru, S. Jaruwatanadilok, and Y. Kuga, *Appl. Opt.* **40**, 5495 (2001).
7. E. E. Gorodnichev, A. I. Kuzovlev, and D. B. Rogozkin, *JETP* **88**, 421 (1999).
8. E. E. Gorodnichev, A. I. Kuzovlev, and D. B. Rogozkin, *Laser Phys.* **9**, 1210 (1999).